ELSEVIER

Journal of Alloys and Compounds 253–254 (1997) 98–100

Journal of ALLOYS AND COMPOUNDS

Hydrogen-induced resistivity increase in amorphous and metastable crystalline (Fe,Co,Ni)–Zr ribbons

J. Tóth*, I. Bakonyi, K. Tompa

Research Institute for Solid State Physics of the Hungarian Academy of Sciences, H-1525 Budapest, P.O.B. 49, Hungary

Abstract

Results of resistivity measurements during electrolytical hydrogen charging on some Fe, Co and Ni based alloy ribbons in amorphous, nanocrystalline and body-centred cubic state are presented. The peculiarities of the H uptake are significantly different for the different structural modifications of alloys with the same chemical composition. In the limited concentration interval of equality of the transferred charge and the number of actually absorbed hydrogen atoms, the concentration variation of the resistivity increment caused by unit hydrogen concentration was determined.

Keywords: Electrolytical hydrogenation; Resistivity increase; Amorphous; Nanocrystalline

1. Introduction

Transport properties very sensitively reflect the presence of hydrogen in metallic glasses. In situ resistivity measurements in the course of the hydrogen charging are used for the investigation of scattering mechanisms of interstitial atoms, for monitoring the structural modifications due to hydrogen absorption and changes in the electronic structure. If the relation between the H concentration and the resistivity once has been determined, the highly accurate measuring possibility of the latter enables us to examine the details of the charging process itself, such as the role of the surface state, the kinetic of the process occurring at the metal–solution interface and rate of the hydrogen diffusion in the bulk of the metal. In this respect, the rather small thickness of melt quenched ribbons is very advantageous because the duration of the diffusion is short and the resistivity value refers to a system with homogeneously distributed hydrogen. The other benefit of the investigation of metal–hydrogen interactions in amorphous alloys is that the amorphous structure could be prepared in a wide concentration interval of its constituents.

2. Experimental details

A melt spinning technique was used to transform the alloys into an amorphous state. Ribbons with the composition $Zr_{10}Fe_{90}$, Zr_9Fe_{91} and Zr_9Co_{91} were easily obtained in amorphous state [1] whereas the structure of melt-quenched Zr–Ni and Hf–Ni ribbons in the vicinity of 90 at.% Ni was strongly dependent on the quenching rate [1,2]. At the highest cooling rate, the alloys $Zr_{10}Ni_{90}$ and Zr_9Ni_{91} could be prepared with an amorphous structure and the alloy $Hf_{11}Ni_{89}$ exhibited a nanocrystalline (nc) phase with the $HfNi_5$ structure whereas at lower quench rates the Zr_9Ni_{91} alloy was prepared as a solid solution of Zr in Ni with a body-centred cubic (bcc) structure. $Zr_{33}Ni_{67}$ and $Zr_{33}Pd_3Ni_{64}$ alloys were melt quenched in an $Ar+H_2$ gas mixture of 1 bar, where the partial pressure of H_2 was ~200 mbar.

Hydrogenation of the ribbons was accomplished at room temperature in 2 volume parts glycerine +1 part phosphoric acid electrolyte at low: $j<1$ mA cm^{-2} current density. Hydrogen charging was performed by applying continuous current charging or by programmed sequential charging current pulses of given length. Hydrogen-content was determined from Faraday's law, the validity of which can be assumed as long as bubble formation on the ribbon is negligible, and this was visually monitored continuously during the charging process.

For the resistance measurements the conventional four-point dc technique was used. Current and potential leads were soft-soldered to two small nickel plates which were preliminary spot welded on both ends of the sample. The measurement of resistance was performed by reversing the measuring current. In this way the direction of the current was opposite in the consecutive time intervals between

*Corresponding author.

0925-8388/97/$17.00
PII S0925-8388(96)02973-8

moments of the resistance measurements. The measuring current was 1 mA and it is known that even higher measuring currents had no influence on charging [3]. The potential drop on the 6 cm long specimen was picked up with a Keithley nanovoltmeter. Immediately before immersing the sample into the electrolyte both sides of it were worked with a fine diamond file until the bright surface of the ''outer'' side of the melt quenched ribbon became matt. The hydrogen charging was performed from both sides of the sample.

3. Results and discussion

In crystalline metals, there exist a few types of sites capable for interstitial H location which are determined by the crystal geometry and by the electronic structure of the neighbouring atoms. The site energies belonging to equivalent sites and the $d\rho/dc_H$ resistivity increment per unit H concentration are independent of the H concentration [4]. So the resistivity is a linear function of the c_H hydrogen concentration and the resistivity increment is given by the slope. But what was said above is valid only in a small interval of H concentration near to zero, because most crystalline metal and alloys react with hydrogen to form metal hydrides. The appearance of a plateau in the pressure–composition isotherm is the unambiguous sign of the hydride formation in crystalline alloys which is absent on the P–C–T curves of their amorphous counterparts [5]. In the concentration interval of hydride formation $d\rho/dc_H$ is drastically different from the value characteristic of the interstitial dissolution [4]. In Fig. 1 for the nc $Hf_{11}Ni_{89}$ alloy the characteristic resistivity increment is 1.2 μΩcm at%$^{-1}$ below ~3 at% hydrogen content. The decrease of the slope is due to bubble formation on the surface of the sample. Some part of the H ions could not get into the bulk of the sample and due to the surface recombination of H to H_2, they form bubbles. In this case the current density j is no longer proportional to the absorbed amount of hydrogen. Because in coulometric charging $c_H \sim j \cdot t$ (t is the duration time of charging), if bubble formation takes place, the real value of the absorbed H is less than the calculated one. Really, in Fig. 1 the declination of the curve correlates with approximately 20% surface coverage by bubbles. (The highly viscous component of the electrolyte has kept the bubbles on the surface throughout the charging process). The first observable bubbles appeared at about 2.5 at% hydrogen content.

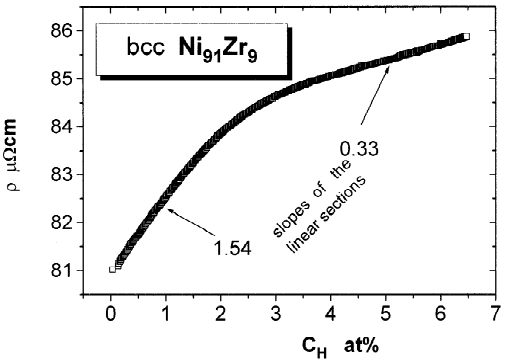

Fig. 2. Increase of the resistivity of a bcc Zr_9Ni_{91} alloy at coulometric hydrogen doping

Figs. 2 and 3 show the resistivity increase for bcc and amorphous Zr_9Ni_{91} alloy respectively. For the bcc structure in the beginning the resistivity increment is 1.5 μΩcm at% H^{-1} without any noticeable bubble formation. But the appearance of the second long linear section—in the presence of a noticeable bubble formation—is surprising, because it can hardly be the result of two completely different compensating processes, namely the result of the continuously increasing number of bubbles (above c_H=6 at% it amounts to 50% surface coverage) and that of the increase of resistivity change per unit H concentration. In Fig. 3, apart from the very low H concentration range (c_H<0.5 at%), for the amorphous Zr_9Ni_{91} alloy 1.02 μΩcm at% H^{-1} resistivity increment was measured up to 4 at% H, where the surface coverage was less than 20%. The measured values of $\Delta\rho/\Delta c_H$ for the initial linear

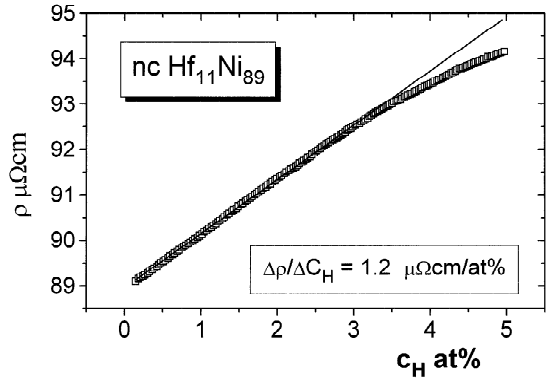

Fig. 1. Increase of the resistivity of a nanocrystalline $Hf_{11}Ni_{89}$ alloy at coulometric hydrogen doping

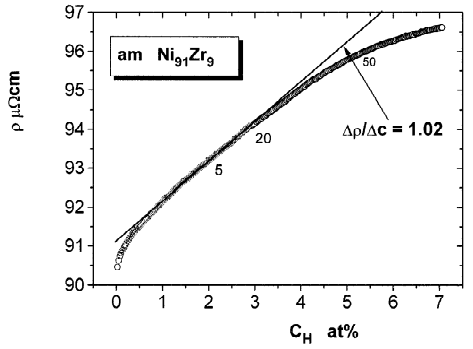

Fig. 3. Increase of the resistivity of an amorphous Zr_9Ni_{91} alloy at coulometric hydrogen doping. The numbers below the curve show the approximate bubble coverage of the surface

Table 1

ALLOY structure	$Hf_{11}Ni_{89}$ nc	Zr_9Fe_{91} am	$Zr_{10}Fe_{90}$ am	Zr_9Co_{91} am	Zr_9Ni_{91} am	Zr_9Ni_{91} am	Zr_9Ni_{91} bcc
$\Delta\rho/\Delta c_H$($\mu\Omega$cm at%$^{-1}$)	1.22	0.30	0.42	0.95	0.57	1.02	1.50
ρ0($\mu\Omega$cm)	89	120	122	100	64	90	81

am: amorphous.

section of the investigated alloys are summarized in Table 1 (ρ_0: resistivity before charging).

All these values are typical for metallic systems, but $\Delta\rho/\Delta c_H$ the resistivity increment is definitely smaller for the Fe–Zr glasses than for the others. Due to the difference of hydride formation enthalpies of Zr and Fe, it may be assumed, that hydrogen first occupies sites in Zr-rich regions. However, at around 90 at% Fe the density of states of Zr–Fe amorphous alloys is characterized [6] by the Fermi level E_F located in the Fe d-band and that of the Zr being slightly above E_F. Therefore, the resistivity of these Zr–Fe alloys is determined by the Fe d-band. In this manner, absorption of H into the Zr-rich regions is expected to influence the resistivity only moderately.

Results for the $Zr_{33}Ni_{67}$ amorphous alloy are strikingly different from all the previous ones. The resistivity increment presented in Fig. 4 is very large, it changes with the H concentration from 5 to 14 $\mu\Omega$cm at% H^{-1}. Some declination on the ρ versus c_H curve appears only above ~20 at% nominal H concentration. Very similar data were measured on a $Zr_{33}Pd_3Ni_{64}$ amorphous alloy, but without any sign of declination on the $d\rho/dc$ versus c_H curve up to the same H content. Previously, results were presented [7] on the resistivity increment of amorphous $Zr_{33}Ni_{67}$ alloy which, however, originated from a different batch. For these samples $\Delta\rho/\Delta c_H$ varied from 1 to 8 $\mu\Omega$cm at%$^{-1}$. The published results for the resistivity increment of $Zr_{33}Ni_{67}$ alloy have already been contradictionary: from [4] $\Delta\rho/\Delta c_H$~0.8–1.2 and from [8] $\Delta\rho/\Delta c_H$ >5 $\mu\Omega$cm at%$^{-1}$. Up to now, an adequate explanation of this discrepancy is not known. However, it is worthwhile to remark that the large value of $\Delta\rho/\Delta c_H$ is accompanied by the large value of the resistivity, which in Ref. [8] and the present work is 220±20 and 234±20, respectively. In all mentioned experiments on amorphous $Zr_{33}Ni_{67}$ alloys, $\Delta\rho/\Delta c$ increases with H content. In Zr–Ni glasses the H atoms enter a few kinds of polyhedra [9] [10], with Zr_4, Zr_3Ni, Zr_2Ni_2 configuration with increasing of site energy. This might be connected with the marked increase of the partial molar volume ΔV of H atom with the hydrogen concentration [11]. The large V(H) is connected with large structural deformations, i.e., causing larger resistivity increase.

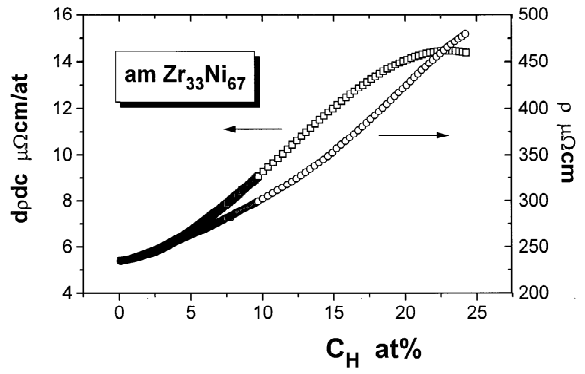

Fig. 4. The dependence of the resistivity increment (left axis) and the resistivity (right axis) on the hydrogen concentration in an amorphous $Zr_{33}Ni_{67}$ alloy

Acknowledgments

This work was supported by the Hungarian Academy of Sciences and by the National Science Foundation under the Grant OTKA T-016670.

References

[1] I. Bakonyi, F. Mehner, M. Rapp, Á. Cziráki, H. Kronmüller and R. Kirchheim, *Z. Metallkde, 86* (1995) 619.
[2] Á. Cziráki, B. Fogarassy, G. Van Tendeloo, P. Lamparter, M. Tegze and I. Bakonyi, *J. Alloys. Comp., 210* (1994) 135.
[3] Á. Szőkefalvy-Nagy, X.Y. Huang and R. Kirchheim, *J. Phys. F, 17* (1987) 427.
[4] B. Chelluri and R. Kirchheim, *J. Non-Cryst. Sol., 54* (1983) 107.
[5] A.J. Maeland, in H. Steeb and H. Warlimont (eds.), *Rapidly Quenched Metals*, North-Holland, Amsterdam, 1985, p. 1507.
[6] I. Turek, Ch. Becker and J. Hafner, *J. Phys.: Cond. Matter, 4* (1992) 7257.
[7] J. Tóth, J. Garaguly, K. Tompa, A. Lovas and L.K. Varga, *Int. Conf. Hydr. Mat. Sci. Katsiveli, Ukraine, 1995*, to be published in *Int. J. Hydrogen Energy*.
[8] A.V. Szafranski and S.M. Filipek, *Z. Phys. Chem. NF, 147* (1986) 15.
[9] T. Araki, T. Abe and K. Tanaka, *Mat. Trans. JIM, 30* (1989) 748.
[10] J.H. Harris, W.A. Curtin and M.A. Tenhover, *Phys. Rev. B, 36* (1987) 5784.
[11] U. Stolz, R. Kirchheim and A. Wildermuth, in S Steeb and H. Warlimont (eds.), *Rapidly Quenched Metals*, North-Holland, Amsterdam, 1985, p. 1537.